Salivary Gland Secretory Carcinoma

Clinicopathologic and Genetic Characteristics of 215 Cases and Proposal for a Grading System

Martina Baněčková, MD, PhD,† Lester D.R. Thompson, MD,‡ Martin D. Hyrcza, MD, PhD,§ Tomáš Vaněček, PhD,‖ Abbas Agaimy, MD, PhD,¶ Jan Laco, MD, PhD,# Roderick H.W. Simpson, MD,** Silvana Di Palma, MD,†† Todd M. Stevens, MD,‡‡ Luka Brcic, MD, PhD,§§ Arghavan Etebarian, DDS, MSc,‖‖ Katarina Dimnik, MD,¶¶ Hanna Majewska, MD,## Ivo Stárek, MD, PhD,*** Esther O'Regan, MD, PhD,††† Tiziana Salviato, MD,‡‡‡ Tim Helliwell, MD,§§§ Markéta Horáková, MD, PhD,*† Wojciech Biernat, MD, PhD,‖‖‖ Timothy Onyuma, MD,¶¶¶ Michal Michal, MD,*† Ilmo Leivo, MD, PhD,### and Alena Skalova, MD, PhD*†*

Abstract: Salivary gland secretory carcinoma (SC), previously mammary analog SC, is a low-grade malignancy characterized by well-defined morphology and an immunohistochemical and genetic profile identical to SC of the breast. Translocation t (12;15)(p13;q25) resulting in the *ETV6*::*NTRK3* gene fusion is a characteristic feature of SC along with S100 protein and mammaglobin immunopositivity. The spectrum of genetic alterations for SC continues to evolve. The aim of this retrospective study was to collect data of salivary gland SCs and to correlate their histologic, immunohistochemical, and molecular genetic data with clinical behavior and long-term follow-up. In this large retrospective study, we aimed to establish a histologic grading scheme and scoring system. A total of 215 cases of salivary gland SCs diagnosed between 1994 and 2021 were obtained from the tumor registries of the authors. Eighty cases were originally diagnosed as something other than SC, most frequently acinic cell carcinoma. Lymph node metastases were identified in 17.1% (20/117 cases with available data), with distant metastasis in 5.1% (6/117). Disease recurrence was seen in 15% (n = 17/113 cases

From the *Department of Pathology, Charles University, Faculty of Medicine in Plzen; †Bioptic Laboratory Ltd Plzen; ‖Molecular Genetic Laboratory, Bioptic Laboratory Ltd, Plzen; #The Fingerland Department of Pathology, Charles University, Faculty of Medicine and University Hospital Hradec Kralove, Hradec Kralove; ***Department of Otorhinolaryngology, University Hospital Olomouc and Faculty of Medicine and Dentistry, Palacky University Olomouc, Olomouc, Czech Republic; ‡Head and Neck Pathology Consultations, Woodland Hills, CA; §Department of Pathology and Laboratory Medicine, University of Calgary, Arnie Charbonneau Cancer Institute; **Department of Pathology and Laboratory Medicine, University of Calgary, Calgary Laboratory Services, Foothills Medical Centre, Calgary, AB, Canada; ¶Institute of Pathology, University Hospital Erlangen, Friedrich-Alexander University Erlangen-Nürnberg (FAU), Comprehensive Cancer Center (CCC) Erlangen-EMN, Erlangen, Germany; ††Division of Clinical Medicine, Department of Histopathology, University of Surrey, Royal Surrey County Hospital, Guildford, Surrey; §§§Department of Cellular Pathology, University of Liverpool, Liverpool, UK; ‡‡‡Department of Pathology, University of Alabama at Birmingham, Birmingham, AL; §§Diagnostic and Research Institute of Pathology, Medical University of Graz, Graz, Austria; ‖‖‖Department of Oral and Maxillofacial Pathology, School of Dentistry, Alborz University of Medical Sciences, Karaj, Iran; ¶¶Institute of Pathology, Faculty of Medicine, University of Ljubljana, Ljubljana, Slovenia; ##Department of Pathology, Warmia and Mazury University, Olsztyn; ‖‖‖‖Department of Pathology, Medical University of Gdansk, Gdansk, Poland; †††Department of Histopathology, St. James's Hospital & Dublin Dental Hospital, Trinity College Dublin, Dublin, Ireland; ‡‡‡Division of Pathology, Department of Medical and Surgical Sciences for Children & Adults, University-Hospital of Modena and Reggio Emilia, Modena, Italy; ¶¶¶Department of Pathology, Kenyatta National Hospital, Nairobi, Kenya; and ###Institute of Biomedicine, Pathology, University of Turku and Turku University Hospital, Turku, Finland.

A.S. and I.L. are senior authors.

All procedures performed in this study involving human participants were in accordance with the ethical standards of the Ethics committee in Pilsen, September 6, 2020, Czech Republic.

The preliminary results of the study were presented as a poster presentation at the United States and Canadian Academy of Pathology's 109th Annual Meeting in Los Angeles, CA, February 29-March 5, 2020.

Conflicts of Interest and Source of Funding: This study was in part supported by study grant SVV 260539 from the Ministry of Education, Czech Republic, the Cooperation Program, research area SURG, the project National Institute for Cancer Research—NICR (Programme EXCELES, ID Project No. LX22NPO5102). Funded by the European Union—Next Generation EU and the Finnish Cancer Society, Finska Läkaresällskapet, and Maritza and Reino Salonen Foundation, Finland. The authors have disclosed that they have no significant relationships with, or financial interest in, any commercial companies pertaining to this article.

Correspondence: Martina Baněčková, MD, PhD, Sikl's Department of Pathology, Medical Faculty of Charles University, Faculty Hospital, E. Benese 13, 305 99 Plzen, Czech Republic (e-mail: baneckova.martina@gmail.com).

Supplemental Digital Content is available for this article. Direct URL citations are provided in the HTML and PDF versions of this article on the journal's website, www.ajsp.com.

with available data). The molecular genetic profile showed *ETV6*::*NTRK3* gene fusion in 95.4%, including 1 case with a dual fusion of *ETV6*::*NTRK3* and *MYB*::*SMR3B*. Less frequent fusion transcripts included *ETV6*::*RET* (n = 12) and *VIM*::*RET* (n = 1). A 3-tiered grading scheme using 6 pathologic parameters (prevailing architecture, pleomorphism, tumor necrosis, perineural invasion (PNI), lymphovascular invasion (LVI), and mitotic count and/or Ki-67 labeling index) was applied. Grade 1 histology was observed in 44.7% (n = 96), grade 2 in 41.9% (n = 90), and grade 3 in 13.5% (n = 29) of cases. Compared with low-grade and intermediate-grade SC, high-grade tumors were associated with a solid architecture, more prominent hyalinization, infiltrative tumor borders, nuclear pleomorphism, presence of PNI and/or LVI, and Ki-67 proliferative index > 30%. High-grade transformation, a subset of grade 2 or 3 tumors, seen in 8.8% (n = 19), was defined as an abrupt transformation of conventional SC into high-grade morphology, sheet-like growth, and a tumor lacking distinctive features of SC. Both overall survival and disease-free survival (5 and 10 y) were negatively affected by tumor grade, stage, and TNM status (each $P < 0.0001$). SC is a low-grade malignancy with predominantly solid-microcystic growth patterns, driven by a gene fusion, most commonly *ETV6*::*NTRK3*. There is a low risk for local recurrence and a good overall long-term survival, with a low risk for distant metastasis but a higher risk for locoregional lymph node metastasis. The presence of tumor necrosis, hyalinization, PNI and/or LVI, and positive resection margins correlate with higher tumor grade, less favorable prognosis, and increased mortality. The statistical results allowed us to design a 3-tiered grading system for salivary SC.

Key Words: secretory carcinoma, salivary gland, *ETV6*::*NTRK3*, grading, overall survival, disease-free survival, hazard ratio

(*Am J Surg Pathol* 2023;47:661–677)

Salivary gland secretory carcinoma (SC) is a low-grade tumor predominantly characterized by a balanced translocation t(12;15)(p13;q25) and *ETV6*::*NTRK3* gene fusion.[1] Salivary SC represents a morphologically and molecularly identical entity when compared with its mammary counterpart.[2] SC was historically categorized as a zymogen granule poor acinic cell carcinoma (AciCC), mucoepidermoid carcinoma, or adenocarcinoma not otherwise specified (NOS).[1] The typical morphology of SC is defined by uniform, eosinophilic, variably vacuolated cells with distinct nucleoli, abundant periodic acid-Schiff (PAS)-positive luminal secretory material, and absence of cytoplasmic zymogen granules. The immunohistochemical (IHC) profile of SC includes positive staining for S100 protein, mammaglobin, CK7, MUC4, and usually SOX10 and GATA3, while DOG1, NOR-1, Nurr1, and p63 are usually negative.[1,3–5]

Although the majority of SCs have an indolent clinical behavior,[1,6] a subset of SCs may exhibit aggressive behavior with a lethal outcome, seemingly related to specific tumor characteristics. In these cases, surgical approaches have limited therapeutic efficacy.[7] For such advanced and surgically unmanageable cases, targeted therapy with tyrosine kinase (NTRK) inhibitors is an alternative treatment option to control the disease.[8,9]

While *ETV6*::*NTRK3* fusion has not been described in any other salivary gland tumors, it is shared with SCs in other anatomic sites including the breast,[2] lacrimal gland,[10] thyroid gland,[11,12] skin,[13–16] sinonasal tract,[17,18] lung,[19] and vulva.[20,21] Still, this fusion is not SC specific, as it is identified in infantile fibrosarcoma,[22] congenital mesoblastic nephroma,[23] hematopoietic malignancies,[24] ALK-negative inflammatory myofibroblastic tumor,[25] gastrointestinal stromal tumor,[26] papillary thyroid carcinoma,[27] and many other entities throughout the body.

Molecular genetics and epigenetics of SC have expanded since the first description of salivary SC in 2010.[1] Ito et al[28] described 2 SCs with a fusion of *ETV6* and a non-*NTRK3* partner, called SCs with *ETV6*::*X* fusion, suggesting a higher malignant potential correlated with their higher grade morphology. In a study of 25 cases, Skálová et al[29] described 5 SCs with alternative breakpoints in *ETV6* and *NTRK3* genes (particularly 4;14 and 5;14) and 4 tumors with *ETV6*::*X* fusion. Subsequently, an *ETV6*::*RET* fusion was identified in 10 cases including the 4 *ETV6*::*X* cases from the previous study.[30] Genetic alterations in *RET* had not been previously described in salivary gland pathology and, importantly, represent an alternative treatment option with a different mechanism of action for targeted therapy in clinically advanced cases.[31] In 1 case of high-grade SC, a new *ETV6* partner was defined by *ETV6*::*MET*.[32] Guilmette et al[33] first described dual pattern fusions with both *ETV6*::*NTRK3* and *ETV6*::*MAML3* identified in the same tumor. Other rare alterations include a *CTNNB1*::*ALK* fusion in a low-grade SC, and a *VIM*::*RET* fusion in a high-grade SC,[34,35] a pathogenic A16V mutation in *PRSS1* gene in 3 low-grade and 5 high-grade SCs, likely pathogenic mutations in *MLH1* and *MUTYH* genes, and a *KMT5A* mutation of uncertain significance in 7 clinically aggressive SCs.[36] As knowledge increases about the genetic findings in SCs, it will further contribute to improving diagnostic procedures, and therapeutic strategies, and potentially predicting clinical behavior.

A few studies have highlighted the prognosis and clinicopathologic features of SC.[6,37–42] To our knowledge, this is the first study to introduce a 3-tiered grading system and scoring system for SC with a correlation to histologic, IHC, molecular genetics, and clinicopathologic data.

MATERIALS AND METHODS

All patients diagnosed with SC recorded between 1996 and 2021 were retrieved from the consultation files of the Salivary Gland Tumor Registry at the Department of Pathology, Faculty of Medicine in Pilsen, Czech Republic, and tumor registries of the co-authors, including SCs with alternative original diagnoses, reclassified after further IHC and molecular genetic testing. Two hundred fifteen cases were selected for further analysis based on the availability of tissue material. Data for evaluation included demographic

information and histopathologic features, including margin status, pattern of growth (microcystic, tubular, solid), infiltration, tumor hyalinization and fibrous septa, tumor necrosis, nuclear pleomorphism (defined as the marked variation in nuclear size and shape), lymphovascular invasion (LVI), perineural invasion (PNI), and mitotic index including Ki-67 labeling index (Table 1, Fig. 1). Mitotic index was determined by counting a total field size of 2 mm^2 (approximately equivalent to 10 HPFs; ×400) in the areas of the highest concentration of mitotic figures (hotspot determination). These parameters were incorporated into a 3-tiered grading system, developed as a risk stratification model to attempt to predict biological behavior and patient outcome independently of age, sex, tumor location, and/or stage. High-grade tumor (HGT) (a subset of grade 2 and 3 tumors) was defined by abrupt transition (dedifferentiation) into high-grade adenocarcinoma or undifferentiated carcinoma.[43,44] In addition, IHC expression of S100 protein, mammaglobin, along with other IHC markers, molecular genetic profile, tumor stage, type of surgery, and adjuvant therapy (including chemotherapy, radiation therapy, proton therapy, and targeted therapy) were tabulated.

Follow-up data were collected from the referring pathologists, clinicians, and hospital charts. The histopathologic features and IHC findings of all tumors were reviewed) to confirm the diagnosis, supported by molecular genetics in 207 cases.[1] The remaining 8 cases lacked material for ancillary testing but fulfilled histologic criteria and immunoprofile (all cases positive for S100 protein and mammaglobin).

This study was approved by the Ethics Committee of the Faculty Hospital in Pilsen and Charles University, Faculty of Medicine in Pilsen, the Czech Republic in 2020.

Histology and IHC

For conventional microscopy, tissues were formalin-fixed and paraffin-embedded (FFPE), sectioned, and stained with hematoxylin and eosin by routine methods.

All primary antibodies used in this study are summarized in (Table 2). For IHC, 4 μm thick sections were cut from paraffin blocks and mounted on positively charged slides (TOMO; Matsunami Glass IND). Sections were processed on a BenchMark ULTRA (Ventana Medical Systems), deparaffinized, and subjected to heat-induced epitope retrieval by immersion in CC1 solution (pH 8.6) at 95°C and for NOR-1 antibody in CC2 solution (pH 6.0) at 92°C. The expression of S100 protein and mammaglobin was stratified according to staining intensity into weak (+), moderate (++), and strong (+++) with at least 10% of the tumor volume showing the reaction.

Molecular Genetic Study

Sample Preparation for Next-generation Sequencing and Reverse Transcription-Polymerase Chain Reaction

For next-generation sequencing (NGS) and reverse transcription-polymerase chain reaction analysis, 2 or 3 FFPE sections (10 μm thick) were macrodissected to isolate tumor-rich regions. Samples were extracted for total nucleic acid using Agencourt FormaPure Kit (Beckman Coulter).

RNA Integrity Assessment and Library Preparation for NGS

Unless otherwise indicated, 250 ng of FFPE RNA was used as an input for NGS library construction. To assess RNA quality, the PreSeq RNA QC Assay using iTaq Universal SYBR Green Supermix (Biorad) was performed

TABLE 1. Histopathologic Parameters in the Proposed Grading System of SC

Parameters	Grade 1	Grade 2	Grade 3*
Morphology and architecture	Predominantly microcystic and tubular with ample secretory material	Solid-cribriform (< 50%), microcystic-cystic, and/or tubulopapillary	• Predominantly solid with minimal or abortive microcystic spaces • Limited secretory material and/or intracytoplasmic vacuoles • Disintegration of tumor cell nests with the production of small tumor buds
Septa, fibrosis, and hyalinization	Lobulated architecture with thin fibrous septa	Abundant fibrous septa with limited/focal hyalinization	• Irregular fibrous septa and/or highly sclerotic
Nucleus and nucleoli	• Regular vesicular nuclei • Fine chromatin • One centrally located nucleolus	• Mild-moderate pleomorphism • Convoluted/wrinkled nuclei often with grooves • One or more small and distinct nucleoli	• Severe pleomorphism • Convoluted/wrinkled hyperchromatic nuclei with occasional nuclear clearing • Multiple nucleoli
Mitoses/2 mm^2	< 3/2 mm^2	3-10/2 mm^2 (nonquantitatively: present, but limited)	≥ 10/2 mm^2 (nonquantitatively: increased) Atypical mitoses
Ki-67 proliferation index	< 15%	15%-31%	≥ 31%
Necrosis	None	Variably present	Present
PNI/LVI	No or limited PNI No LVI	Present PNI and/or LVI (but not common)	Present
Infiltration	Circumscribed, focally encapsulated	Circumscribed, not encapsulated, with invasion	Destructively invasive

*High-grade transformation is part of the grade 3 category, but with more sheet-like growth and comedonecrosis.

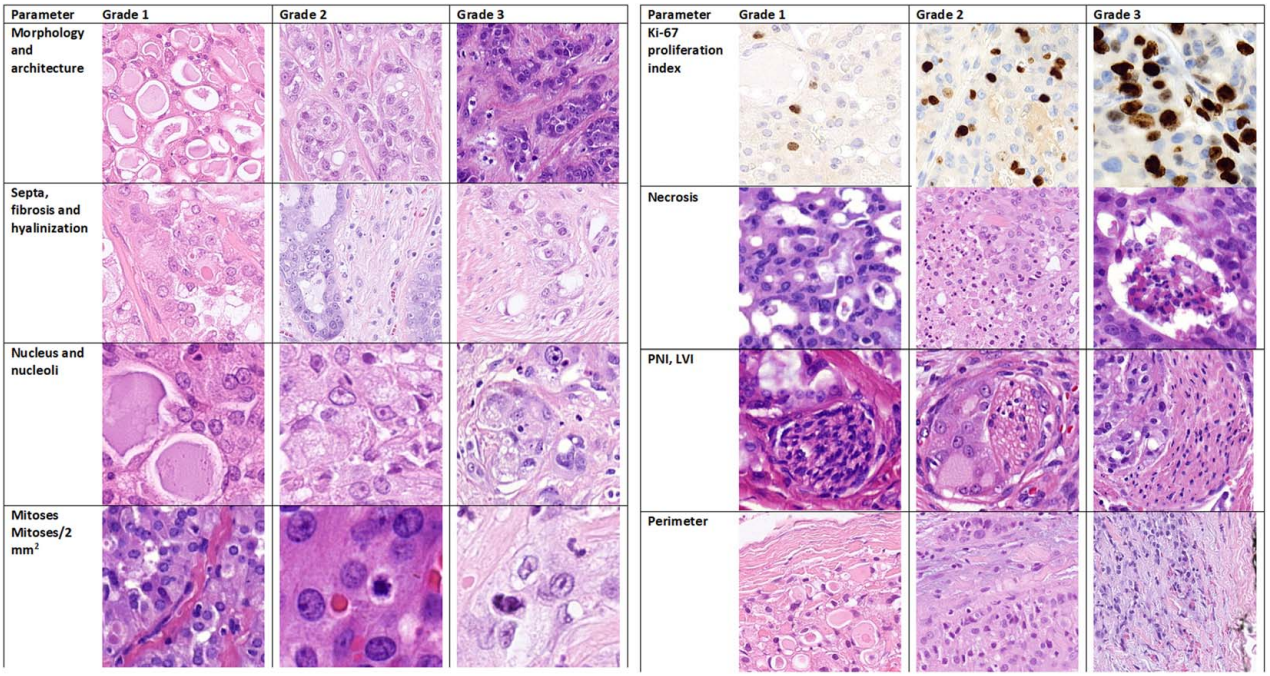

FIGURE 1. Histopathologic parameters used in a proposed grading scheme of SC—graphic documentation corresponds to Table 1.

on all samples during library preparation to generate a measure of the integrity of RNA (in the form of a cycle threshold [C_t] value). Library preparation and RNA QC were performed following the Archer FusionPlex Solid Tumor Kit for Illumina (ArcherDX Inc.), as previously described.[30] Final libraries were diluted 1:100,000 and quantified in a 10 µL reaction following the Library Quantification for Illumina Libraries protocol and assuming a 200 bp fragment length (KAPA). The concentration of final libraries was around 200 nM. The threshold representing the minimum molar concentration for which sequencing can be robustly performed was set at 50 nM.

NGS and Analysis

Libraries were diluted to 4 nM and sequenced on a NextSeq sequencer (Illumina). The optimal number of raw reads per sample was set to 3 million. Library pools were diluted to 1.6 pM library stock with 20% 1.8 pM PhiX and loaded in the NextSeq cartridge. The fusion and other rearrangement detection algorithm of Archer Analysis rely on the specificity of the gene-specific primers used in the amplification steps in the AMP process. The resulting FASTQ files were analyzed using the Archer Analysis software (version 5.1.7; ArcherDX Inc.).

Detection of Alterations in *ETV6*, *NTRK3*, and *RET* Genes by Fluorescence In Situ Hybridization Method

Four-microliter-thick FFPE sections were placed onto positively charged slides. Hematoxylin and eosin–stained slides were examined for the determination of areas for cell counting. The unstained slides were routinely deparaffinized and incubated in the ×1 Target Retrieval Solution Citrate at pH 6 (Dako) and at 95°C for 40 minutes and subsequently cooled for 20 minutes at room temperature in the same solution. Slides were washed in deionized water for 5 minutes and digested in protease

TABLE 2. Antibodies Used for IHC Study

Antibody specificity	Clone	Dilution	Antigen retrieval/time	Source
S-100 protein	Polyclonal	RTU	EnVision High pH/30 min	Dako
Mammaglobin	304-1A5	RTU	EnVision High pH/30 min	Dako
CK7	OV-TL 12/30	RTU	EnVision High pH/30 min	Dako
p63	DAK-p63	RTU	EnVision Low pH/30 min	Dako
DOG-1	SP31	RTU	CC1/36 min	Cell Marque
NOR-1	H-7	1:50	CC2/68 min	Ventana
GATA-3	L50-823	1:200	CC1/52 min	BioCareMedical
SOX 10	SP267	RTU	CC1/64 min	Cell Marque
Ki-67	MIB-1	RTU	EnVision High pH/30 min	Dako

CC1 indicates EDTA buffer pH 8.6 at 95°C; CC2, citrate buffer pH 6.0 at 92°C; EnVision High pH 9.0 at 97°C; EnVision Low pH 6.0 at 97°C; RTU, ready to use.

TABLE 3. Overall Clinicopathologic Data for 215 Cases of Salivary Gland SC

Attribute	N = 215, n (%)
Sex	
Male	123 (57.2)
Female	87 (40.5)
Unknown	5 (2.3)
Age (y)	
Average	47.5
Median	48.5
Range	7-94
Size (mm)	
≤20	130 (60.5)
20-40	50 (23.3)
>40	9 (4.2)
Unknown	26 (12.1)
Average	19.8
Median	15
Range	4-70
Location	
Parotid gland	159 (74.0)
Submandibular gland	14 (6.5)
Lip	12 (5.6)
Buccal mucosa	10 (4.7)
Palate	10 (4.7)
Oral cavity (NOS)	5 (2.3)
Sinonasal tract	5 (2.3)
Initial diagnosis	
SC	132 (61.4)
AciCC	34 (15.8)
Adenocarcinoma	12 (5.6)
Mucoepidermoid carcinoma	9 (4.2)
Polymorphous adenocarcinoma	10 (4.7)
Intraductal carcinoma or salivary duct carcinoma	8 (3.7)
Metastasis of renal cell carcinoma	4 (1.9)
Other	6 (2.8)
Margins	
Free	55 (25.6)
Close (<1 mm)	62 (28.8)
Involved	64 (29.8)
Unknown	34 (15.8)
Infiltrative growth	
Encapsulated/circumscribed	58 (27.0)
Circumscribed but infiltrative	85 (39.5)
Destructively infiltrative	64 (29.8)
Perineural invasion	
Case number	47 (21.9)
LVI	
Case number	41 (19.1)
Tumor grade	
1	96 (44.7)
2	90 (41.9)
3	29 (13.5)
High-grade transformation	19 (8.8)
Follow-up (mo)	
Average	66.8
Median	48
Range	2-600
n (average) (%)	
Alive without disease	91 (73.5) (42.8)
Died of disease	5 (35.2) (2.3)
Alive with disease	5 (43.4) (2.3)
Died of unrelated reasons	8 (44.0) (3.3)
Lost to follow-up or unknown	106 (49.3)
Treatment	
Parotidectomy (not specified)	30 (14.0)
Superficial/partial parotidectomy	20 (9.3)
Total parotidectomy	8 (3.7)
Local tumor excision	52 (24.2)
Wide local excision	22 (10.2)
Lymph node dissection	21 (9.8)
Radiotherapy	37 (17.2)
Chemotherapy	4 (1.9)
Larotrectinib/STARTRK2 trial	1/1 (0.5/0.5)
Proton therapy	1 (0.5)
Declined	3 (1.4)
Unknown	79 (36.7)
Recurrence*	
Yes	17 (14.9)
No	96 (44.7)
Unknown	102 (47.4)
Median to recurrence (mo)	24
Average to recurrence (mo)	69.7
T classification	
1	129 (60.0)
2	48 (22.3)
3	6 (2.8)
4	7 (3.3)
Unknown	25 (11.6)
N classification†	
0	97 (82.9)
1	10 (8.5)
2a	0 (0.0)
2b	10 (8.5)
Unknown	98 (50.2)
Lymph node involvement†	
No. patients	20 (17.1)
Median (mo)	16
Average (mo)	33.8
Distant metastasis†	
0	120 (55.8)
1	6 (5.1)
Unknown	90 (41.9)
Median to metastasis (mo)	29
Average to metastasis (mo)	121.3
AJCC stage group	
I	126 (58.6)
II	43 (20.0)
III	8 (3.7)
IVA	11 (5.1)
IVB	2 (0.9)
IVC	1 (0.5)
Unknown	24 (11.2)
Molecular findings	
ETV6 break	18 (8.4)
ETV6::NTRK3	176 (81.9)
ETV6::RET	12 (5.6)
VIM::RET	1 (0.5)
Not performed	8 (3.7)

*Data available in 113 cases and percentages of known cases were calculated accordingly.

†Data available in 117 cases and percentages of known cases were calculated accordingly.

solution with pepsin (0.5 mg/mL; Sigma Aldrich) in 0.01 M HCl at 37°C for 25 to 60 minutes, according to the sample conditions. Slides were then placed into deionized water for 5 minutes, dehydrated in a series of ethanol solutions (70%, 85%, 96% for 2 min each), and air-dried.

Two commercial probes were used for the detection of rearrangement of *ETV6* and *RET* genes, Vysis ETV6 Break Apart FISH Probe Kit (Vysis/Abbott Molecular, IL) and ZytoLight SPEC RET Dual Color Break Apart Probe (ZytoVision GmbH). The *ETV6* probe was mixed with

TABLE 4. Proposed Scoring System for Each Tumor Grade of SC

	Feature point score = 1	Feature point score = 2	Feature point score = 3
Architecture	No solid component and or presence of fibrous septae	Solid component <50% sclerosis might be present	Predominantly solid with loss of tumor cell cohesion and/or prominent sclerosis
Nuclei	Monomorphic	Mild pleomorphism	Pleomorphic
PNI, LVI, necrosis	None	PNI and/or necrosis (*no LVI*)	LVI (*PNI or necrosis might be present*)
Mitotic activity/ Ki-67 proliferation index	$<3/2$ mm^2 and/or <15%	3-10/2 mm^2 and/or 15%-31%	$\geq 10/2$ mm^2 and/or $\geq 31\%$

Grade 1: Total score = 4 to 6.
Grade 2: Total score = 7 to 9.
Grade 3: Total score = 10 to 12.
$P < 0.0001$ (log-rank test) for OS and DFS.

water and LSI/WCP (Locus-Specific Identifier/Whole Chromosome Painting) Hybridization buffer (Vysis/Abbott Molecular) in a 1:2:7 ratio, respectively. The *RET* probe was factory premixed. Probes for the detection of rearrangement of the *NTRK3* gene region were mixed from custom-designed SureFISH probes (Agilent Technologies Inc.). Chromosomal regions for *NTRK3* break-apart probe oligos are chr15:87501469-88501628 and chr15:88701444-89700343. The probe mixture was prepared from the corresponding probes (each color was delivered in a separate well), deionized water, and LSI Buffer (Vysis/Abbott Molecular) in a 1:1:1:7 ratio, respectively.

An appropriate amount of mixed and premixed probes was applied to the specimens, covered with a glass coverslip, and sealed with rubber cement. Slides were incubated in the ThermoBrite instrument (StatSpin/Iris Sample Processing) with codenaturation at 85°C for 8 minutes and hybridization at 37°C for 16 hours. The rubber cemented coverslip was then removed and the slide was placed in a posthybridization wash solution (2 × SC/0.3% NP-40) at 72°C for 2 minutes. The slide was air-dried in the dark, counterstained with 4′,6′-diamidino-2-phenylindole DAPI (Vysis/Abbott Molecular), cover slipped, and examined immediately.

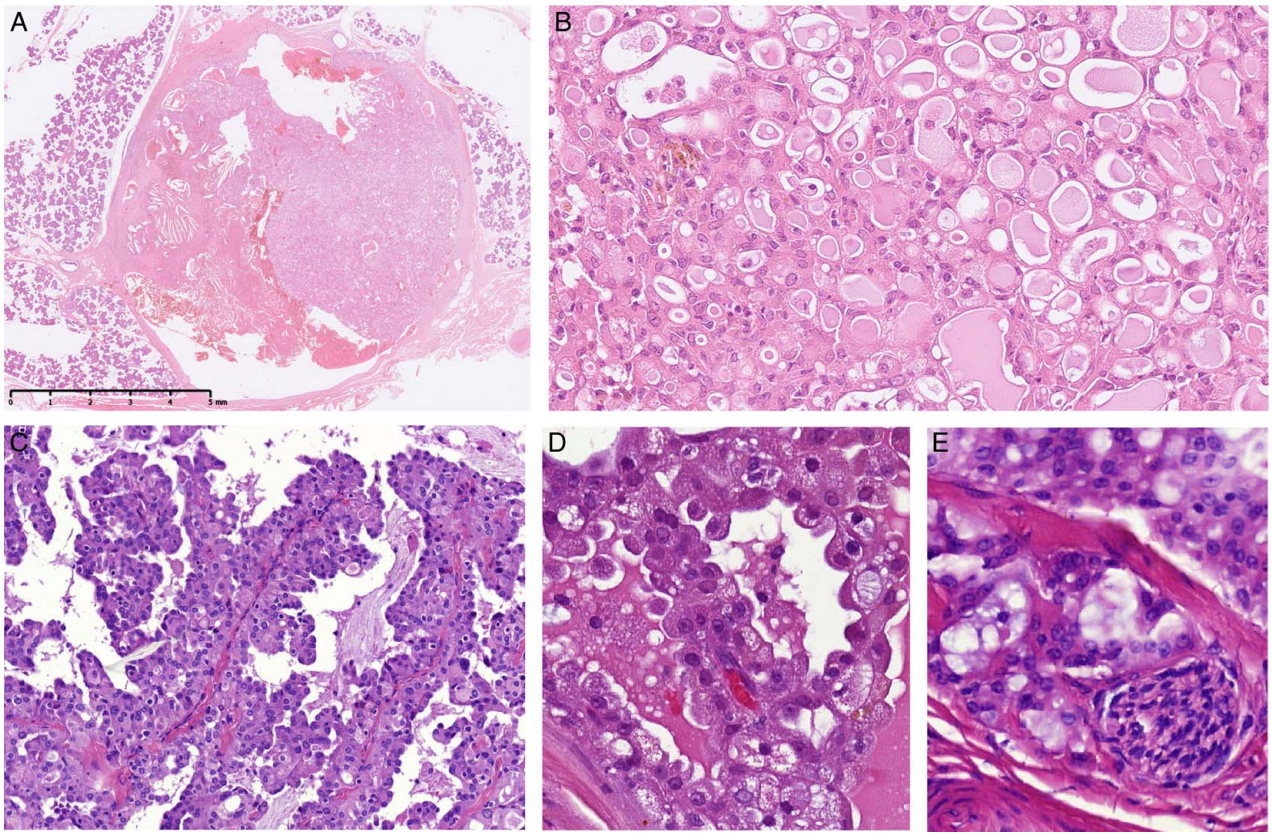

FIGURE 2. Grade 1 tumors were well circumscribed and encapsulated with cystic transformation (A). Tumors were lobulated, with nests separated by fibrous septa, showing microcystic or tubular growth with eosinophilic intraluminal material (B). Some cases displayed papillary architecture (C) with hobnail cells (D). PNI was detected infrequently (E).

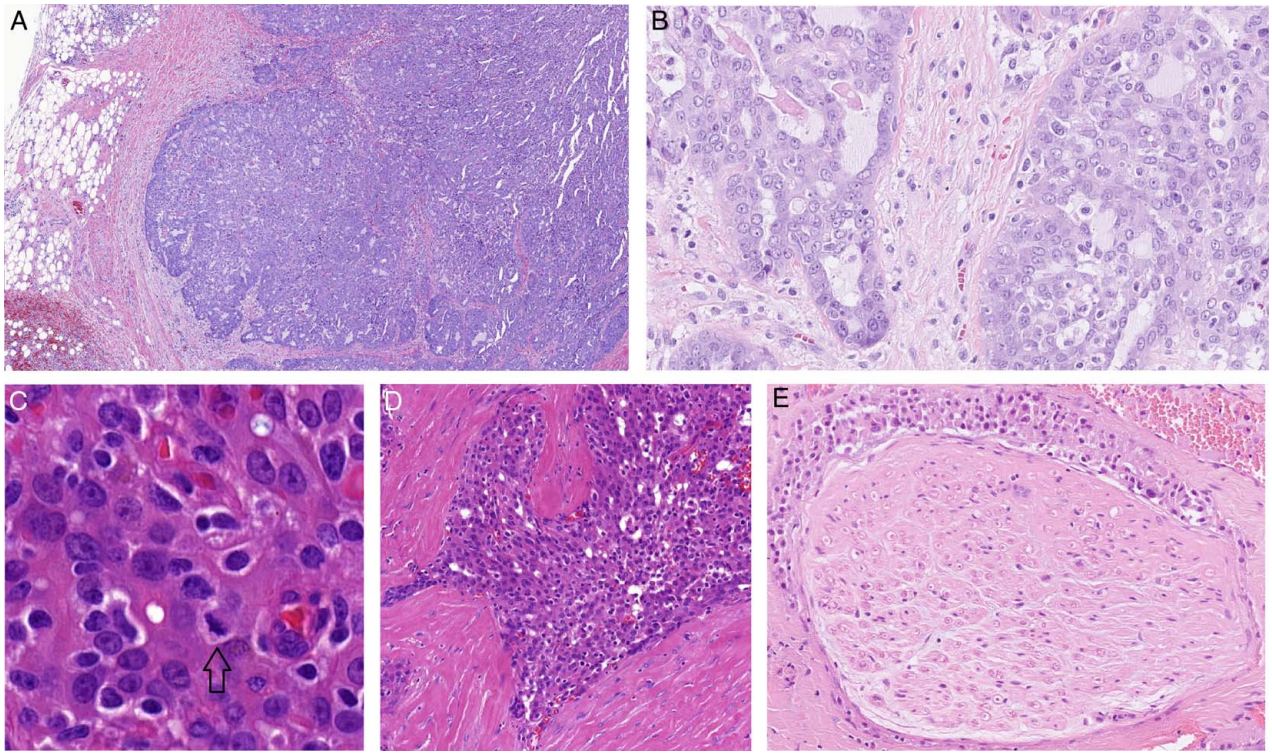

FIGURE 3. Grade 2 tumors were circumscribed but not encapsulated and often showed invasive fronds (A). They grew in solid, cribriform, or papillary patterns often with microcystic spaces (B). The nuclei were created with mild-to-moderate pleomorphism, nuclear grooves, and 1 or more enlarged eosinophilic nucleolus; few mitoses were present (*arrow*) (C). Some areas were more solid with prominent sclerosis (D) and often PNI (E).

Fluorescence In Situ Hybridization Interpretation

The sections were examined with an Olympus BX51 fluorescence microscope (Olympus Corporation) using a ×100 objective and filter sets Triple Band Pass (DAPI/SpectrumGreen/SpectrumOrange), Dual Band Pass (SpectrumGreen/SpectrumOrange), and Single Band Pass (SpectrumGreen or SpectrumOrange). For each probe, 100 randomly selected nonoverlapping tumor cell nuclei were examined for the presence of yellow, green or orange fluorescent signals. As regards the break-apart probe, yellow signals were considered negative, and separate orange and green signals were considered as positive. Cut-off values for the break-apart probes were set at $>10\%$ of nuclei with chromosomal breakpoint signals, (mean + 3 SD in normal non-neoplastic control tissues).

Statistics Description

Statistical analysis was performed using SW SAS.

The descriptive statistics such as absolute and relative frequencies, mean, SD, variance, median, interquartile range, minimum, and the maximum was calculated.

The significance of observed differences in proportions was tested using the χ^2 test and Fisher exact test. The clinical importance of examined factors was evaluated by odds ratio calculations.

The Kaplan-Meier analyses were used to calculate overall survival (OS), time to first metastases, and disease-free survival (DFS). The Gehan Wilcoxon test, log-rank test, and Cox regression hazard model including hazard ratio (HR) calculations were used to assess the clinical impact of examined covariates and multivariate analysis. The C & RTs (classification and regression tree) was calculated for the respective endpoints of OS and DFS. All survival graphs have been performed by SW Statistica (StatSoft Inc.). Statistical significance was determined at the level of 5%.

RESULTS

Clinicopathologic Characteristics of Patient and Tumor Variables

A total of 215 patients were included. Detailed clinical characteristics and demographics are summarized in Table 3. Of 215 cases, 83 (38.6%) were originally diagnosed as AciCC (n = 34), adenocarcinoma, NOS (n = 12), mucoepidermoid carcinoma (n = 9), polymorphous adenocarcinoma (n = 10), intraductal carcinoma or salivary duct carcinoma (n = 8), metastatic renal cell carcinoma (n = 4), and others (n = 6). Fifty-nine cases were previously included in other studies.[18,29,30,35,45–48]

The average age at presentation was 47.5 years (range: 7 to 94 y) affecting 123 males and 87 females (1.4:1), without data in 5 cases. The most commonly affected site was the parotid gland (n = 159), followed by the submandibular gland (n = 14), lip (n = 12), buccal mucosa (n = 10), palate (n = 10), oral cavity, NOS (n = 5),

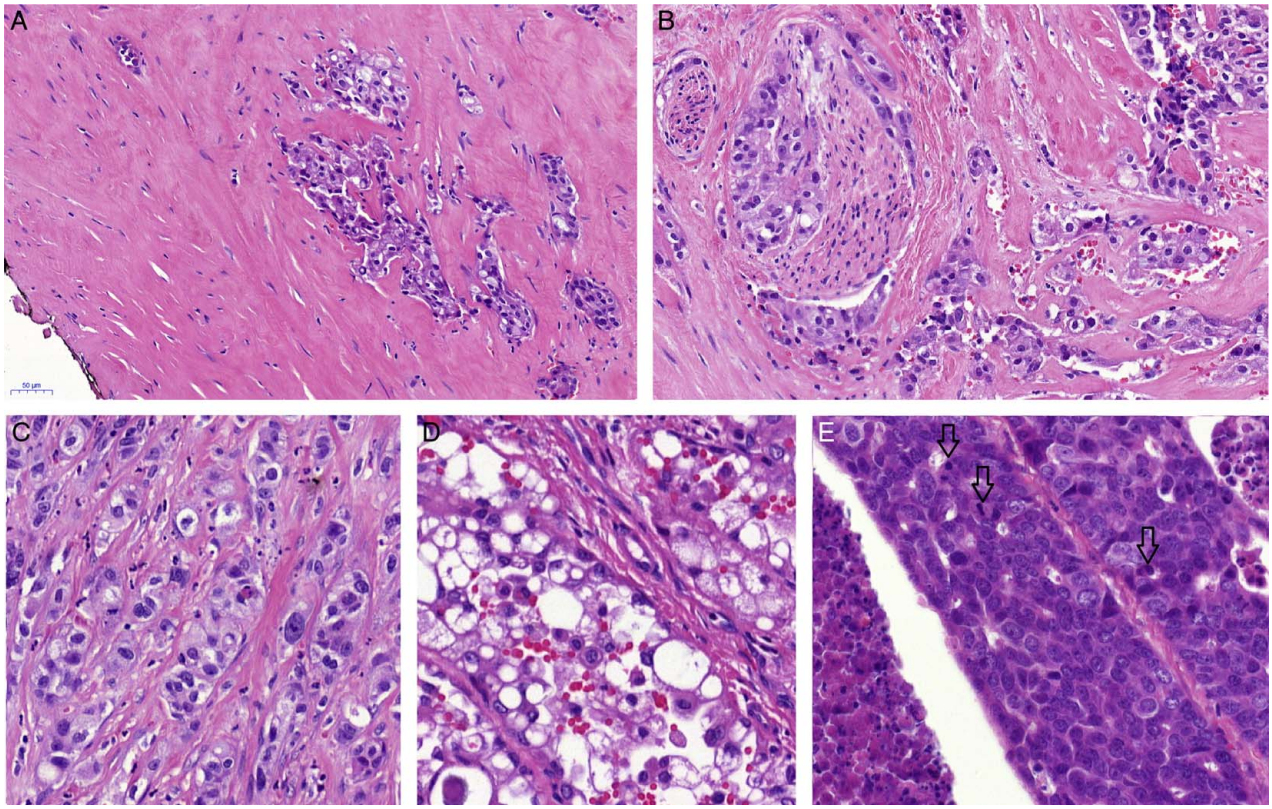

FIGURE 4. Grade 3 tumors were unencapsulated with invasive growth and prominent sclerosis (A). The tumor cells showed solid growth with no or minimal microcystic spaces and a tendency to split in small tumor buds; PNI was present in almost all cases (B). Some areas were more trabecular, with significant nuclear pleomorphism (C). Clear cell features were focally noted (D). Mitoses (*arrows*) and tumor necrosis were prominent (E).

and sinonasal tract (n = 5). The average size was 19.8 mm (median: 15 mm, range: 4 to 70 mm). Presenting symptoms included swelling or slowly growing tumor mass (n = 70), facial nerve palsy (n = 5), aggressive and rapid growth, skin infiltration, and neck lymphadenopathy (n = 5). The average symptom duration was 24.8 months (range: 1 to 276 mo). Fifteen patients developed additional unrelated neoplasms: thyroid tumor (n = 4), lymphoma/leukemia (n = 3), breast carcinoma (n = 2), colorectal carcinoma (n = 1), or another head and neck tumor (n = 5), but none were part of a genetic predisposition tumor syndrome.

Surgical treatment was considered complete microscopically in 117 patients (54%), including 55 cases with tumor-free margins and 62 cases with tumor cells present within 1 mm (close) from the margin. Microscopic involvement of the resection margin was reported in 64 cases (30%), including 12 patients treated by a wide excision or total parotidectomy, 30 patients treated by simple excision/superficial or partial parotidectomy/parotidectomy, NOS, and unknown in the remaining patients.

Treatment, Tumor Behavior, and Follow-up

Treatment, tumor behavior, and follow-up was available in 136 cases (Table 3). Surgery was performed in 132 cases, while declined by 3 patients. Parotidectomy was performed in 58, superficial or partial parotidectomy in 20, total parotidectomy in 8, and parotidectomy NOS in 30 patients, respectively. In locations other than the parotid gland, wide (complete) tumor excision was performed in 22 and local tumor excision in 52 patients, respectively. Adjuvant radiation, chemotherapy, and/or proton therapy followed surgical treatment in 37, 4, and 1 patient, respectively). One patient was treated with larotrectinib and 1 was admitted to the STARTRK2 trial (a basket study of entrectinib [RXDX-101], for the treatment of patients with solid tumors harboring *NTRK1/2/3* [Trk A/B/C], *ROS1*, or *ALK* gene rearrangements). Lymph node dissection was performed in 21 patients). Local recurrence developed in 17 of 114 patients (average: 69.7 mo, median: 24 mo). Regional lymph node metastases were detected in 20 of 117 patients (average: 33.8 mo; median: 16 mo; range: 7 to 86 mo) after diagnosis. Distant metastases occurred in 6 of 117 patients, to bone, lung, pleura, pericardium, and skin (average: 121 mo; median: 29 mo; range: 7 to 588 mo).

Complete follow-up was available in 109 patients (51%; Table 3). The average follow-up time was 66.8 months (median: 48 mo; range: 2 to 600 mo). The majority of patients were alive without evidence of disease (n = 91 with an average follow-up of 73.5 mo (range: 2 to 600 mo). Five patients were alive with the disease

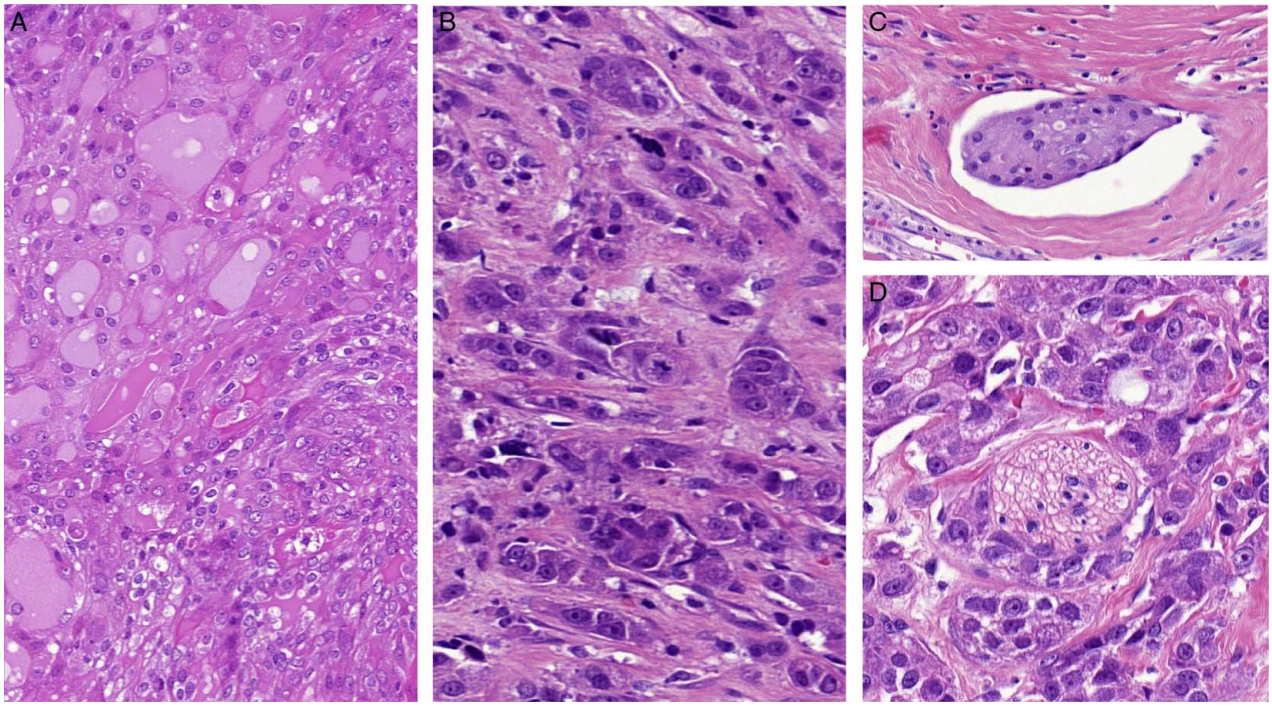

FIGURE 5. High-grade transformation was defined as abrupt transformation of conventional SC (*left*) into high-grade morphology that lacks original distinctive features of SC (*right*) (A). The character of growth and nuclei in high-grade areas was grade 3 with severe nuclear pleomorphism and many mitoses (*arrow*) (B). LVI (C) and PNI (D) were present in almost all cases.

(average: 43.4 mo; range: 24 to 60 mo). Five patients died of disease (average: 35.2 mo; range: 11 to 79 mo), while 8 patients died of unrelated causes (average: 44 mo; range: 18 to 120 mo).

TNM categories and staging groups are detailed in Table 3. Overall, pT was predominantly low with pT1 (n = 129) and pT2 (n = 48) accounting for 93% of all patients; pT3 (n = 6) and pT4 (n = 7) were uncommon, with pT group unavailable in 25 patients). Lymph nodes were evaluated in 117 patients: 97 patients (82.9%) were free of tumor, and 20 patients (17.1%) developed lymph node metastases: 10 patients had metastasis in a single ipsilateral lymph node ≤ 3 cm in greatest dimension (pN1); 10 patients had multiple ipsilateral lymph nodes affected (pN2b). Distant metastases (M1) were reported in 6 of 117 patients (5.1%). Staging, performed using the American Joint Committee on Cancer (AJCC) eighth edition, was documented in 191 patients: stage I: n = 126; stage II: n = 43; stage III: n = 8; stage IVA: n = 11; stage IVB: n = 2; stage IVC: n = 1.

Grading and Risk Stratification

Cases were stratified according to the proposed grading system based on a literature of potentially negative prognostic histologic factors already reported. The proposed grading criteria include tumor perimeter, histologic growth pattern, fibrous septa/fibrosis and/or stromal hyalinization, PNI, LVI, tumor necrosis, nuclear pleomorphism and nucleolar morphology, and mitotic activity and/or Ki-67 labeling index (Table 1, Fig. 1). Similar parameters have been selected in other salivary gland grading schemata,[49–53] but weighted based on severity or extent of the feature present in an increasing point system, with 1 to 3 points assigned based on presence, extent or quantitative increased in the parameter. Using these features, tumors were separated into 3 grades, recognizing that HGT is a unique subset of grade 3 tumors, as many of the parameters identified in the areas of HGT show grade 3 parameters. Each tumor was categorized into 3 grades (Table 4) using the proposed scoring system (grade 1 = score 4 to 6; grade 2 = score 7 to 9; grade 3 = score 10 to 12). Each grade was statistically evaluated in univariate and multivariate analysis with a *P*-value <0.05 considered statistically significant.

Grade 1 tumors were well circumscribed and encapsulated to partially with minimal invasive growth. A cystic appearance (Fig. 2A) was common. Tumors were lobulated, composed of nests separated by fibrous septa with microcystic or tubular growth patterns and production of PAS-positive secretory material (Figs. 2A, B). Fibrosis was mild to moderate. In some cases, there was papillary architecture with hobnail cells (Figs. 2C, D). The nuclei were round to oval and regular with vesicular, delicate chromatin and one centrally located nucleolus. Mitoses, PNI, or LVI were present only sporadically (Fig. 1, 2E), if at all when the entire tumor was evaluated (ie, not evaluated on a core needle or incisional biopsy). Tumor necrosis was absent.

Grade 2 tumors were circumscribed but not encapsulated and often showed invasive fronds (Fig. 3A). They

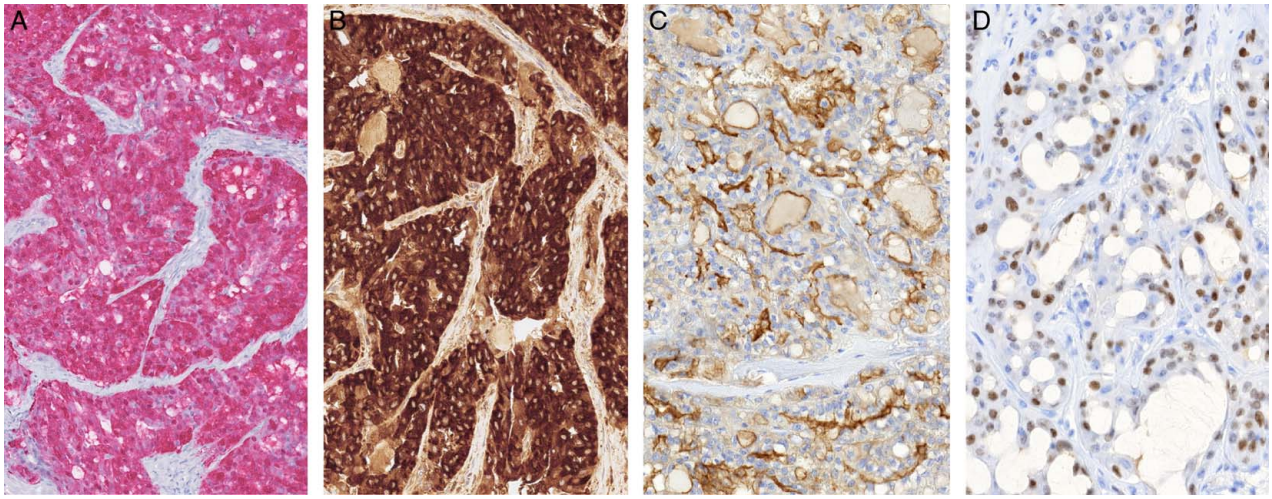

FIGURE 6. Almost all cases expressed S100 protein (A) and mammaglobin (B). DOG1 is nearly always negative, but a single grade 3 tumor showed strong (luminal/membranous) DOG1 immunoexpression (C). One case of grade 2 showed nuclear p63 expression in 60% of tumor cells (D).

grew in solid, cribriform, or papillary patterns often with microcystic spaces and production of PAS-positive, occasionally bluish material (Fig. 3B). Cystic architecture with papillary projections was present but reduced in frequency. An apocrine tumor cell morphology was identified in a few cases. The nuclei were folded with mild to intermediate pleomorphism, nuclear grooves, and 1 or more enlarged eosinophilic nucleolus (Fig. 3C). Mitotic index contained >3 but <10 mitoses/2 mm^2 (Fig. 3C). Fibrosis/sclerosis was heavier and demonstrated wider septa, with PNI usually easily noted, while LVI was present, but generally not affecting many vessels (Figs. 3D, E). Tumor necrosis was frequently present, but not in large geographic regions (Fig. 1).

Grade 3 tumors were destructively invasive, mostly solid with absent or limited microcystic spaces (Fig. 4A). Some cases showed disintegration of tumor cell nests resulting in presence of tumor buds (nests of <10 tumor cells), or single cells embedded in a desmoplastic stroma (Fig. 4B). These tumors were highly sclerotic (Fig. 4A). Nuclei were markedly pleomorphic and bizarre (Fig. 4C). Some cases showed

TABLE 5. Correlation of Specific Variables With Tumor Grade (Univariate Analysis)

		n (%)				
Statistical variables	**Groups**	**Grade 1 (N = 96)**	**Grade 2 (N = 90)**	**Grade 3 (N = 29)**	***P***	**Odds ratio (CI range)**
Hyalinization and sclerosis	None to mild	64 (67)	38 (42)	8 (28)	<0.0001	2.515 (1.642-3.850)
	Intermediate and strong	30 (31)	51 (57)	21 (72)		
Infiltration	Noninvasive (circumscribed and encapsulated)	39 (41)	19 (21)	0 (0)	<0.0001	3.754 (2.135-6.692)
	Invasive (circumscribed but invasive and destructively invasive)	51 (53)	69 (77)	29 (100)		
PNI	Not identified	90 (94)	64 (71)	11 (38)	<0.0001	5.782 (3.229-10.352)
	Identified	4 (4)	25 (28)	18 (62)		
LVI	Not identified	91 (95)	69 (77)	11 (38)	<0.0001	6.697 (3.573-12.554)
	Identified	3 (3)	20 (22)	18 (62)		
Necrosis	Not identified	94 (98)	77 (86)	11 (38)	<0.0001	14.222 (6.141-32.936)
	Identified	0 (0)	12 (13)	18 (62)		
Statistical variable	Period	Grade 1	Grade 2	Grade 3	*P*	HR (CI range)
Metastasis	None in 1-y period	100%	100%	80.00%	<0.0001	6.412 (2.208-18.612)
	None in 5-y period	100%	89.84%	35.00%		
	None in 10-y period	90.00%	89.84%	35.00%		

TABLE 6. OS and DFS by Selected Parameters

	OS				DFS			
Variables	5-y period	10-y period	Long-rank test *P*	HR (CI range)	5-y period	10-y period	Long-rank test *P*	HR (CI range)
Grade (G)	G1: 97.6% G2: 82.8% G3: 62.8%	G1: 97.6% G2: 82.8% G3: 31.4%	0.0001	4.823 (2.071-11.231)	G1: 89.6% G2: 75.9% G3: 20.0%	G1: 80.6% G2: 69.6% G3: 20.0%	0.0001	3.733 (2.098-6.642)
AJCC stage	I: 97.8% II: 89.1% III: 40.0% IV (A-B): 58.3%	I: 97.8% II: 89.1% III: 40.0% IV (A-B): 0.0%	0.0001	3.033 (1.806-5.093)	I: 86.1% II: 82.9% III: ≤20.0% IV (A-B): ≤14.3%	I: 81.3% II: 82.9% III: 0.0% IV (A-B): 0.0%	0.0001	2.856 (1.934-4.216)
TNM stage (T category)	T1: 97.9% T2: 90.6% T3: 25.0% T4: 50.0%	T1: 97.9% T2: 80.6% T3: ≤25.0% T4: ≤50.0%	0.0001	3.604 (2.044-6.353)	T1: 86.5% T2: 79.7% T3: ≤20.0% T4: 14.3%	T1: 74.5% T2: 79.7% T3: ≤20.0% T4: ≤14.3%	0.0001	2.532 (1.687-3.799)
Age (y)	<55: 97.9% ≥55: 72.0%	<55: 97.9% ≥55: 64.0%	0.0002	16.787 (2.166-13.111)	<50: 90.2% ≥50: 63.1%	<50: 79.0% ≥50: 58.9%	0.0001	3.974 (1.344-11.750)
Sex (M: male; F: female)	M: 83.4% F: 92.7%	M: 78.8% F: 92.7%	0.1103	3.209 (0.702-14.661)	M: 70.7% F: 82.2%	M: 61.8% F: 82.2%	0.0818	6.590 (2.427-0.894)

nuclear clearing (Fig. 4D). Nucleoli were often multiple and macronucleoli. Tumor necrosis was prominent and frequently geographic. There was easily identified and increased foci PNI and/or LVI (both within and beyond the tumor), while mitoses were increased at $>10/2$ mm^2 and/or $>31\%$ Ki-67 labeling index (Figs. 1, 4B, 4E). HGT was detected by the abrupt transition of conventional SC into high-grade morphology that lacked any of the distinctive SC features (Figs. 5A–D).

IHC Findings

All cases with available material were investigated immunohistochemically for S100 protein and mammaglobin (Figs. 6A, B). S100 protein was positive in all 206 cases (96%) tested. Strong expression was observed in 137 cases (66.5%), moderate intensity in 48 cases (23.3%), and weak intensity in 19 cases (9.2%) (2 cases were not scored because slides were unavailable). Mammaglobin was detected in 195 cases (from 197 cases (92%) with available tissue block), with strong expression in 150 cases (76.9%), moderate in 16 (8.2%), weak in 22 (11.3%) and 7 (3.6%) not scored as slides were unavailable. Mammaglobin was negative in 2 cases, both with *ETV6*::*NTRK3* fusion. DOG1 was tested in 147 cases (68%): 127 (115.7%) were negative, and 20 (13.6%) were positive with weak intensity (Fig. 6C). NOR1 (NR4A3) was negative in all cases tested (n = 73, 34%). p63 was evaluated in 178 cases (83%): negative in 152 (85.4%) cases and in 26 cases (14.6%) was focally positive in the basal zone only (Fig. 6D).

The correlation of grading/risk stratification of SC to clinicopathologic and morphologic variables is explained in Supplementary Table 1 (Supplemental Digital Content 1, http://links.lww.com/PAS/B530).

Molecular Genetic Findings

All cases were investigated by fluorescence in situ hybridization, reverse transcription-polymerase chain reaction, and/or NGS. The *ETV6*::*NTRK3* gene fusion was detected in 176 cases (81.8%) (including 1 case with a dual fusion of *ETV6*::*NTRK3* and *MYB*::*SMR3B)*, *ETV6*::*RET* fusion in 12 cases (5.6%), and *VIM*::*RET* fusion in 1 case (0.5%). Eighteen cases (8.4%) showed only *ETV6* break by fluorescence in situ hybridization and without sufficient material could not be tested by other methods. Four cases failed analysis and 4 cases lacked material for testing (each 1.8%).

Statistical Analysis

The various histologic parameters were separately investigated as potential predictors of grade and patient outcome (DFS vs. OS; Table 5).

The mean time to metastasis was 80.4 months (SD = 0.2 mo). Tumor grade was closely associated with the risk for distant metastasis. In grade 2 and 3 tumors, a shorter time was documented to develop distant metastases than in grade 1 tumors (log-rank test $P<0.0001$). The risk was estimated by the regression hazard model to be 6.4 ($P=0.0006$).

OS and DFS in relation to different variables and HRs are cataloged in Table 6. OS was determined by the number of patients who died of disease, were alive with disease, died of other causes, and were alive with no evidence of disease. The average survival was 73 months (SD = 0.15 mo) (Fig. 7A). HR for tumor grade showed that patients with grade 3 tumors had 4.82 times greater

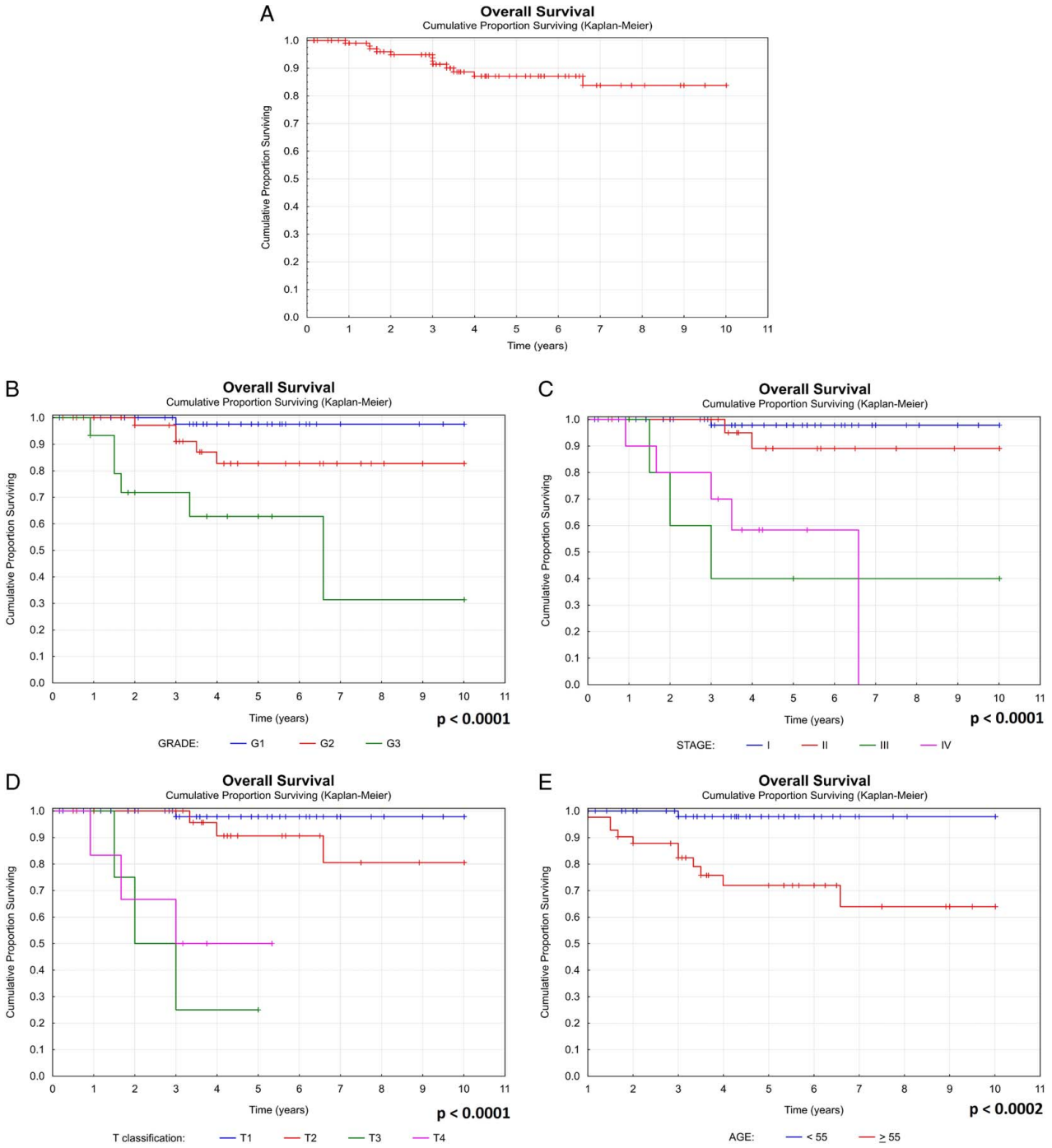

FIGURE 7. OS of SC by Kaplan-Meier univariate analysis (A). Overall survival of SC related to tumor grade (B), tumor stage (C), tumor size (D), and patient age (E). All P < 0.0002.

risk of dying from the disease ($P < 0.0001$) (Fig. 7B). The higher the AJCC stage was the worse the OS became (3.03 times, $P < 0.0001$) (Fig. 7C). An increase of the pT stage (TNM classification) by one step was associated with 3.60 times greater mortality due to disease ($P < 0.0001$) (Fig. 7D). The age cutoff for an increased risk of worse outcome was > 55 years (HR = 16.787, $P < 0.0002$) (Fig. 7E). Sex did not have a significant impact on survival ($P = 0.1103$), but male patients had a lower 5-year (83.4%) and 10-year (78.8%) OS when compared with female patients (5- and 10-y survivals were equal at 92.7%). Males had 3.21 times greater risk of dying from the disease. The tumor site did not have a significant impact on OS ($P = 0.1323$).

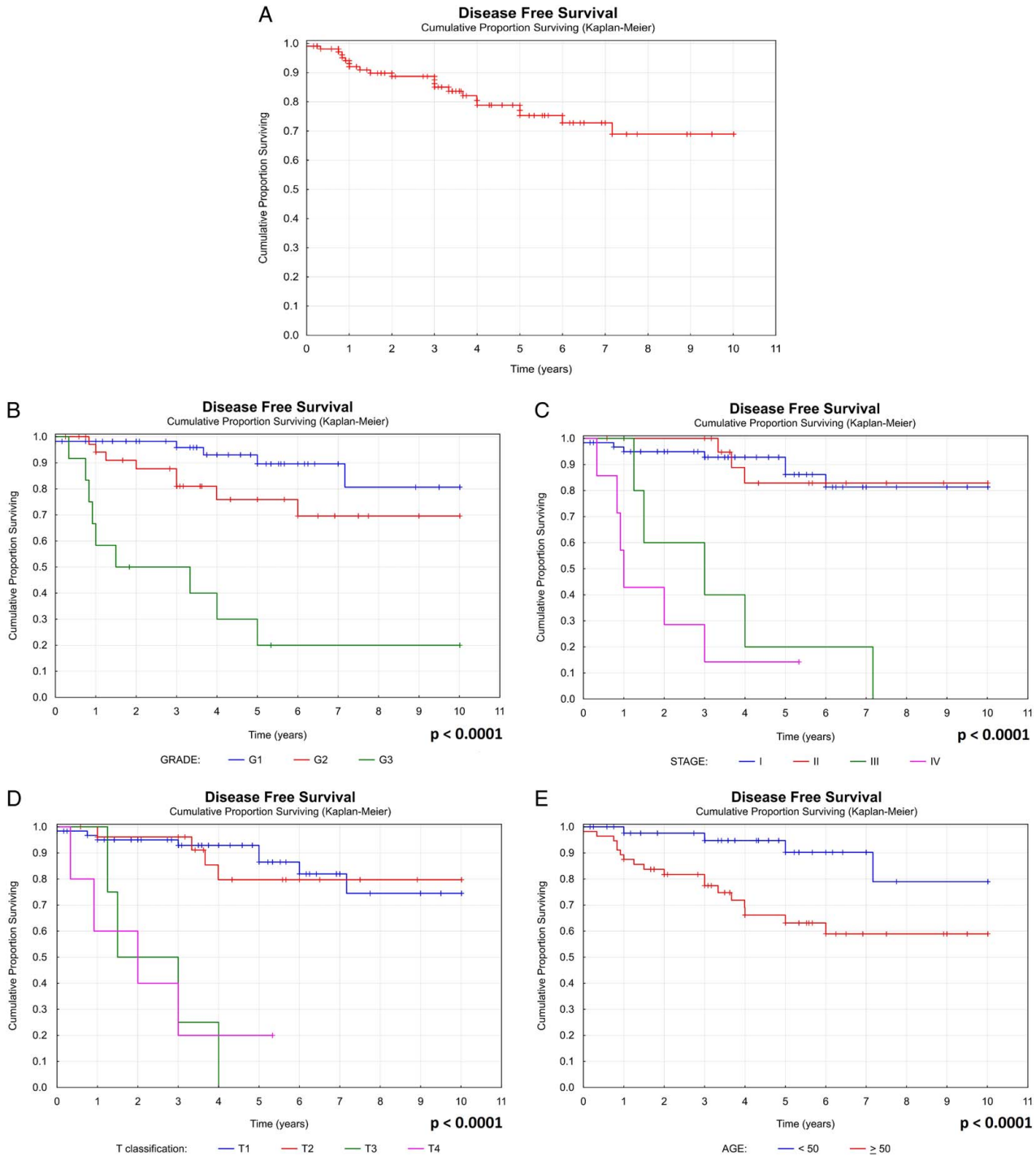

FIGURE 8. DFS of SC by Kaplan-Meier univariate analysis (A). DFS of SC related to tumor grade (B), tumor stage (C), tumor size (D), and patient age (E). All $P < 0.0001$.

DFS was determined from the date of primary treatment to the time of development of lymph node metastasis, recurrence, distant metastasis, patient's death of other causes, or being alive with no evidence of disease. The average survival was 72 months (SD = 0.23 mo) (Fig. 8A). DFS was influenced by tumor grade, as grade 3 tumors had 3.73 times greater risk of causing death from disease ($P < 0.0001$) (Fig. 8B). The higher the AJCC stage was the shorter was DFS, with each step of higher grade decreasing the DFS by 2.76 times ($P < 0.0001$) (Fig. 8C). The higher the pT stage (TNM classification) the greater mortality due to disease was 2.53 times ($P < 0.0001$) (Fig. 8D). Increased risk of death occurred statistically above the age of 50 years (HR = 3.97, $P < 0.0001$)

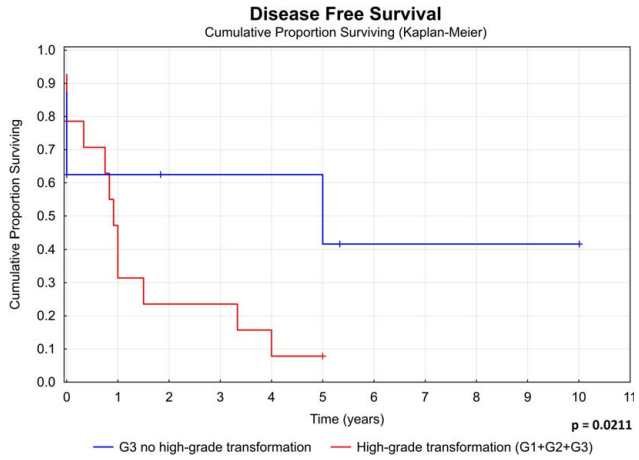

FIGURE 9. DFS by Kaplan-Meier univariate analysis for tumors with and without high-grade transformation (data available for DFS only as there was no event in one of the groups in the OS calculation, P=0.0211).

(Fig. 8E). Sex did not have a statistically significant impact on survival ($P = 0.0818$), although females had a higher 5- and 10-year survival (both 82.2%), while males had a 5-year survival of 70.7% and 10-year survival of 61.8%. Males had 6.69 times higher likelihood of negative events. Tumor site did not have a significant impact on DFS ($P = 0.1393$).

Patients without HGT (including grade 3 patients) had 8.3 times lower risk of recurrence and/or death from the disease when compared with patients with HGT (grade 2 and 3 in our series) ($P = 0.0497$, CI = 1.003-68.732) (Fig. 9). This parameter was available for DFS only, as there was no event in one of the groups in the OS calculation (Cox proportional hazards model).

Multivariate survival analysis using Cox proportional hazards model was applied on the proposed scoring system and its variables (architecture, nuclear pleomorphism, presence of PNI/LVI/necrosis and MIB1/Ki-67 index), the stratification of score into grade 1 = score 4 to 6; grade 2 = score 7 to 9; grade 3 = score 10 to 12) was statistically significant with $P < 0.0001$ for OS and DFS (Figs. 10A, B).

Multivariate analysis identified 3 prognostic factors for OS: pT stage (T3+T4; HR = 34.5; CI = 1.198-991.457; $P = 0.0389$), location (parotid site; HR = 25.98; CI = 1.333-506.471; $P = 0.0316$), and score (score 10 to 12; HR = 21.2; CI = 1.117-400.676; $P = 0.0420$) (Fig. 11A). Regression tree analysis ranked the factors for OS in order of significance, with pT stage being the most significant and scoring system being the second most significant (Supplementary Table 2, Supplemental Digital Content 2, http://links.lww.com/PAS/B531).

There were 2 independent predictors of DFS, in a particular stage (stage III+IV, HR = 22.1; CI = 2.992-163.354; $P = 0.0024$) and score (score 10 to 12; HR = 6.3; CI = 1.686-23.710; $P = 0.0063$) (Fig. 11B). Regression tree analysis ranked the factors for OS in order of significance, with pT stage being the most significant and grade being the second most significant (Supplementary Table 2, Supplemental Digital Content 2, http://links.lww.com/PAS/B531).

DISCUSSION

Demographic Analysis and Histologic Impact on Tumor Grade

SC has been recognized as a distinct entity since 2010[1] and included in the fourth edition of the World Health Organization Classification of Head and Neck Tumours.[54] Previously, SC was usually classified as zymogen granule poor AciCC, which remains the greatest mimic of SC.[55] Demographically, AciCCs are more frequent in females,[56,57] whereas SC has a male predominance (this report shows a male to female ratio of 1.4:1).

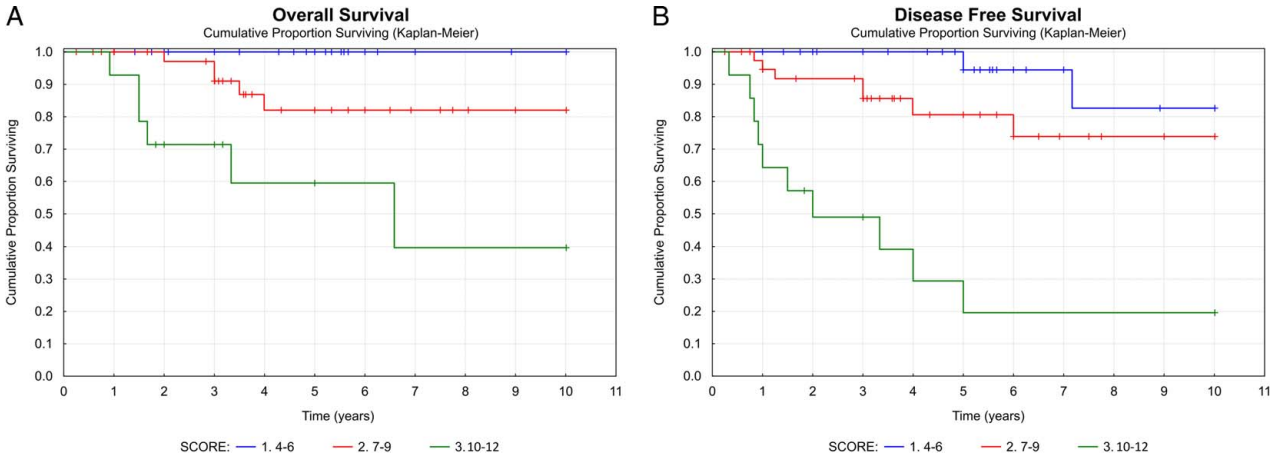

FIGURE 10. OS of SC by Kaplan-Meier multivariate analysis which emphasized that OS decreases with an increasing number of independent risk factors, including pT3+4 stage, parotid location, and score 10 to 12 (A). DFS of SC by Kaplan-Meier multivariate analysis which emphasized that DFS decreases with an increasing number of risk factors including pT 3+4 stage and score 10 to 12 (B). Both $P < 0.0001$.

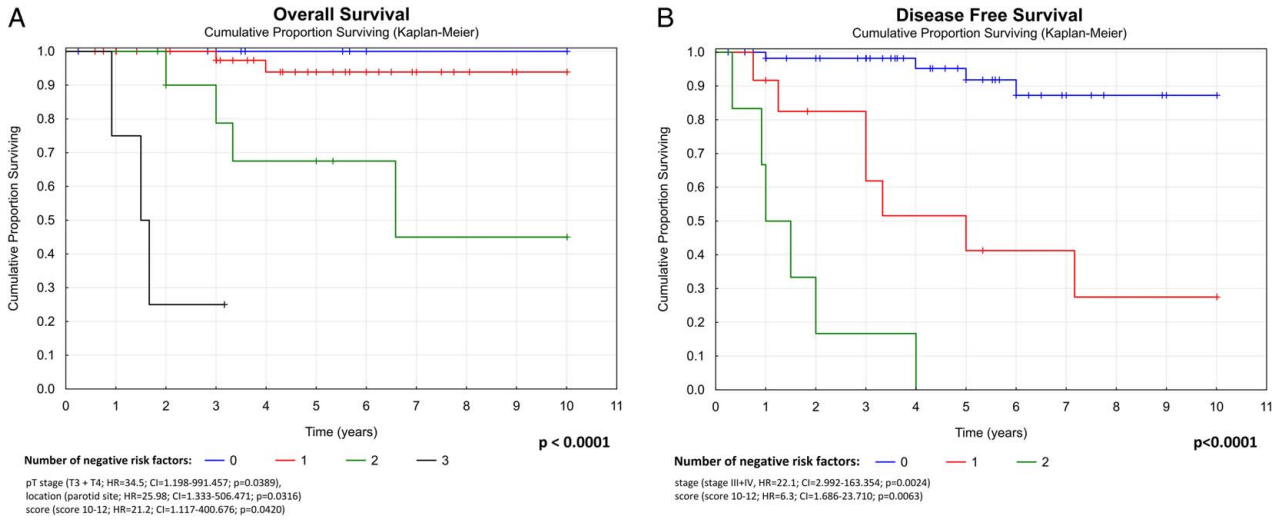

FIGURE 11. Regression tree analysis ranked the factors for OS in order of significance, with pT stage being the most significant and score being the second most significant (A), similarly for DFS pT stage being the most significant factor and grade being the second most significant (B). Both $P < 0.0001$.

Earlier reports suggested that SC is more frequently localized in nonparotid gland sites,[6,58] but our findings and those of others show parotid gland predilection.[40]

The clinical behavior of both SC and AciCC is predominantly low grade. However, lymph node metastasis in SC was reported by Chiosea et al[6] at 17.6% of cases in contrast to AciCC at 7.9% and 10% in the series of van der Poorten et al.[55] The present study is in line with previous reports, showing a 17.1% rate of lymph node metastasis. The risk for distant spread in AciCC is considered to have a HR of 7.50 by Patel et al.[56] In SC, the present report estimated an HR of 6.4 for distant metastasis.

Grading of SC was not suggested until the recent paper by Xu et al.[41] These authors proposed a 2-tiered grading system, based on mitotic count and the presence of necrosis. Tumors with <5 mitoses/10 HPF and no tumor necrosis were graded as low-grade SC and tumors with ≥5 mitoses/10 HPF and/or necrosis were evaluated as high-grade SC. The authors performed a multivariate survival analysis and identified mitotic index, LVI, nuclear pleomorphism, and high-grade transformation as independent prognostic factors for DFS. Necrosis and tumor infiltration were not statistically significant.

Based on our observations we suggest a 3-tiered grading system for SC featuring 4 histologic parameters: (1) architecture and fibrous septae/fibrosis; (2) nuclear pleomorphism; (3) PNI, LVI, and tumor necrosis; (4) and mitotic activity/Ki-67 index. Each parameter is scored on a 1 to 3 scale and aggregated to yield a final grade: grade 1 = score 4 to 6, grade 2 = score 7 to 9, and grade 3 = score 10 to 12.

Survival Analysis

Only a few studies have provided OS and DFS in SC patients.[6,37,38,41,59] Boon et al[37] reported a larger cohort of 31 cases with 5- and 10-year OS of 95%, and 5- and 10-year DFS of 89%. These findings correspond to our data for grade 1 or 2 cases, while data for grade 3 cases were different as those authors did not evaluate HGTs. Similarly, the study by Ayre et al[38] showed 5- and 10-year DFS of 96% and 85%, respectively, but only for conventional SCs (low grade), although grade was not specifically addressed. Xu et al[41] described 5- and 10-year DFS as 93% and 73% for low-grade lesions and 46% and 46% for high-grade SCs, although absolute criteria may not have been similar to what is presented herein.

We report a dramatic decrease in the survival of patients with clinically advanced and histologically aggressive disease. Patients with grade 1 and 2 tumors had 10-year OS of 97.6% and 82.8%, and DFS of 80.6% and 69.6%, respectively. Patients with grade 3 tumors had 10-year OS of 31.4% and DFS of 20%. Patients with grade 3 tumors had 4.82 times greater risk of dying from the disease. A 5-year OS in grade 1 and 2 tumors was the same as 10-year survival, but in grade 3 tumors OS was 62.8%. A 5-year DFS in grade 1 and 2 tumors was 89.6% and 75.9%, respectively, while for grade 3 tumors it was identical to a 10-year DFS.

Tumor size affected both OS and DFS. A larger tumor size (pT) resulted in a dramatic decrease in the survival of patients, and they had 3.60 times greater risk of dying from the disease. Patients with tumor size <20 mm (pT1) and 20 to 40 cm (pT2) had a 10-year OS survival of 97.9% and 89.1%, respectively, which decreased markedly when tumor size exceeded >4 cm (pT3) or there was skin invasion (pT4), respectively. In pT3 and pT4, 10-year OS was ≤25% and ≤50%, respectively. DFS in a 10-year period showed an increase of negative events with larger tumors: DFS was 74.5% in pT1 and 14.3% for pT4 (HR = 2.53).

These data suggest that better OS and DFS are seen in females with lower stages, small tumor size, and grades 1 and 2 tumors without the presence of high-grade transformation.

Study Limitations

This is a retrospective study of 215 SC cases. However, complete follow-up was not available in nearly half of the cases. For purposes of statistical testing, we revised the number of cases and performed the calculations using the actual numbers of available cases for each variable. The mean survival time and its SE were underestimated because the largest observation was censored, and the estimation was restricted to the largest event time. Another study limitation is that the majority of the cases are from consultations, which may introduce a bias towards more aggressive cases. Nevertheless, only 18 cases had been submitted with a diagnosis of high-grade carcinoma (mostly salivary duct carcinoma or metastasis from primary locations other than salivary glands). Despite limitations, this study has analyzed one of the largest patient cohorts to date and provided insights into the clinical behavior of SC.

CONCLUSIONS

The proposed grading system of SC as correlated to histologic findings and clinical behavior has shown value in relationship to OS and DFS, along with other prognostic findings related to TNM staging, age, and genetic sex. The differences between grades 1, 2, and 3 from a histologic and also prognostic perspective are statistically significant, with *P*-values of all mentioned variables <0.0001 (Tables 5, 6). Thus, SC grading is recommended to help risk stratify patients and potentially guide therapy.

ACKNOWLEDGMENTS

The authors thank engineer Stanislav Kormunda for statistical processing.

REFERENCES

1. Skalova A, Vanecek T, Sima R, et al. Mammary analogue secretory carcinoma of salivary glands, containing the ETV6-NTRK3 fusion gene: a hitherto undescribed salivary gland tumor entity. *Am J Surg Pathol*. 2010;34:599–608.
2. Tognon C, Knezevich SR, Huntsman D, et al. Expression of the ETV6-NTRK3 gene fusion as a primary event in human secretory breast carcinoma. *Cancer Cell*. 2002;2:367–376.
3. Haller F, Bieg M, Will R, et al. Enhancer hijacking activates oncogenic transcription factor NR4A3 in acinic cell carcinomas of the salivary glands. *Nat Commun*. 2019;10:368.
4. Haller F, Moskalev EA, Kuck S, et al. Nuclear NR4A2 (Nurr1) immunostaining is a novel marker for acinic cell carcinoma of the salivary glands lacking the classic NR4A3 (NOR-1) upregulation. *Am J Surg Pathol*. 2020;44:1290–1292.
5. Taverna C, Baneckova M, Lorenzon M, et al. MUC4 is a valuable marker for distinguishing secretory carcinoma of the salivary glands from its mimics. *Histopathology*. 2021;79:315–324.
6. Chiosea SI, Griffith C, Assaad A, et al. Clinicopathological characterization of mammary analogue secretory carcinoma of salivary glands. *Histopathology*. 2012;61:387–394.
7. Skalova A, Vanecek T, Majewska H, et al. Mammary analogue secretory carcinoma of salivary glands with high-grade transformation: report of 3 cases with the ETV6-NTRK3 gene fusion and analysis of TP53, beta-catenin, EGFR, and CCND1 genes. *Am J Surg Pathol*. 2014;38:23–33.
8. Kummar S, Lassen UN. TRK inhibition: a new tumor-agnostic treatment strategy. *Target Oncol*. 2018;13:545–556.
9. Drilon A. TRK inhibitors in TRK fusion-positive cancers. *Ann Oncol*. 2019;30:viii23–viii30.
10. Hyrcza MD, Andreasen S, Melchior LC, et al. Primary secretory carcinoma of the lacrimal gland: report of a new entity. *Am J Ophthalmol*. 2018;193:178–183.
11. Reynolds S, Shaheen M, Olson G, et al. A case of primary mammary analog secretory carcinoma (MASC) of the thyroid masquerading as papillary thyroid carcinoma: potentially more than a one off. *Head Neck Pathol*. 2016;10:405–413.
12. Dogan S, Wang L, Ptashkin RN, et al. Mammary analog secretory carcinoma of the thyroid gland: a primary thyroid adenocarcinoma harboring ETV6-NTRK3 fusion. *Mod Pathol*. 2016;29:985–995.
13. Kazakov DV, Hantschke M, Vanecek T, et al. Mammary-type secretory carcinoma of the skin. *Am J Surg Pathol*. 2010;34:1226–1227; author reply 1228.
14. Hyrcza MD, Ng T, Crawford RI. Detection of the ETV6-NTRK3 translocation in cutaneous mamary-analogue secretory carcinoma. *Diagn Histopathol*. 2015;21:481–484.
15. Bishop JA, Taube JM, Su A, et al. Secretory carcinoma of the skin harboring ETV6 gene fusions: a cutaneous analogue to secretory carcinomas of the breast and salivary glands. *Am J Surg Pathol*. 2017;41:62–66.
16. Kastnerova L, Luzar B, Goto K, et al. Secretory carcinoma of the skin: report of 6 cases, including a case with a novel NFIX-PKN1 translocation. *Am J Surg Pathol*. 2019;43:1092–1098.
17. Lurquin E, Jorissen M, Debiec-Rychter M, et al. Mammary analogue secretory carcinoma of the sinus ethmoidalis. *Histopathology*. 2015;67:749–751.
18. Baneckova M, Agaimy A, Andreasen S, et al. Mammary analog secretory carcinoma of the nasal cavity: characterization of 2 cases and their distinction from other low-grade sinonasal adenocarcinomas. *Am J Surg Pathol*. 2018;42:735–743.
19. Huang T, McHugh JB, Berry GJ, et al. Primary mammary analogue secretory carcinoma of the lung: a case report. *Hum Pathol*. 2018;74:109–113.
20. Nguyen JK, Bridge JA, Joshi C, et al. Primary mammary analog secretory carcinoma (MASC) of the vulva with ETV6-NTRK3 fusion: a case report. *Int J Gynecol Pathol*. 2019;38:283–287.
21. Baban F, Shah K, Torres-Mora J, et al. Secretory carcinoma (mammary analogue secretory carcinoma) of the vulva with ETV6 gene rearrangement: a brief report with follow-up. *Int J Gynecol Pathol*. 2021;40:e2–e3.
22. Knezevich SR, Garnett MJ, Pysher TJ, et al. ETV6-NTRK3 gene fusions and trisomy 11 establish a histogenetic link between mesoblastic nephroma and congenital fibrosarcoma. *Cancer Res*. 1998;58:5046–5048.
23. Knezevich SR, McFadden DE, Tao W, et al. A novel ETV6-NTRK3 gene fusion in congenital fibrosarcoma. *Nat Genet*. 1998;18:184–187.
24. Kralik JM, Kranewitter W, Boesmueller H, et al. Characterization of a newly identified ETV6-NTRK3 fusion transcript in acute myeloid leukemia. *Diagn Pathol*. 2011;6:19.
25. Yamamoto H, Yoshida A, Taguchi K, et al. ALK, ROS1 and NTRK3 gene rearrangements in inflammatory myofibroblastic tumours. *Histopathology*. 2016;69:72–83.
26. Atiq MA, Davis JL, Hornick JL, et al. Mesenchymal tumors of the gastrointestinal tract with NTRK rearrangements: a clinicopathological, immunophenotypic, and molecular study of eight cases, emphasizing their distinction from gastrointestinal stromal tumor (GIST). *Mod Pathol*. 2021;34:95–103.
27. Leeman-Neill RJ, Kelly LM, Liu P, et al. ETV6-NTRK3 is a common chromosomal rearrangement in radiation-associated thyroid cancer. *Cancer*. 2014;120:799–807.
28. Ito Y, Ishibashi K, Masaki A, et al. Mammary analogue secretory carcinoma of salivary glands: a clinicopathologic and molecular study including 2 cases harboring ETV6-X fusion. *Am J Surg Pathol*. 2015;39:602–610.
29. Skalova A, Vanecek T, Simpson RH, et al. Mammary analogue secretory carcinoma of salivary glands: molecular analysis of 25 ETV6 gene rearranged tumors with lack of detection of classical ETV6-NTRK3 fusion transcript by standard RT-PCR: report of 4 cases harboring ETV6-X gene fusion. *Am J Surg Pathol*. 2016;40:3–13.

30. Skalova A, Vanecek T, Martinek P, et al. Molecular profiling of mammary analog secretory carcinoma revealed a subset of tumors harboring a novel ETV6-RET translocation: report of 10 cases. *Am J Surg Pathol*. 2018;42:234–246.
31. Li AY, McCusker MG, Russo A, et al. RET fusions in solid tumors. *Cancer Treat Rev*. 2019;81:101911.
32. Rooper LM, Karantanos T, Ning Y, et al. Salivary secretory carcinoma with a novel ETV6-MET fusion: expanding the molecular spectrum of a recently described entity. *Am J Surg Pathol*. 2018;42: 1121–1126.
33. Guilmette J, Dias-Santagata D, Nose V, et al. Novel gene fusions in secretory carcinoma of the salivary glands: enlarging the ETV6 family. *Hum Pathol*. 2019;83:50–58.
34. Sasaki E, Masago K, Fujita S, et al. Salivary secretory carcinoma harboring a novel ALK fusion: expanding the molecular characterization of carcinomas beyond the ETV6 gene. *Am J Surg Pathol*. 2020;44:962–969.
35. Skalova A, Baneckova M, Thompson LDR, et al. Expanding the molecular spectrum of secretory carcinoma of salivary glands with a novel VIM-RET fusion. *Am J Surg Pathol*. 2020;44:1295–1307.
36. Na K, Hernandez-Prera JC, Lim JY, et al. Characterization of novel genetic alterations in salivary gland secretory carcinoma. *Mod Pathol*. 2020;33:541–550.
37. Boon E, Valstar MH, van der Graaf WTA, et al. Clinicopathological characteristics and outcome of 31 patients with ETV6-NTRK3 fusion gene confirmed (mammary analogue) secretory carcinoma of salivary glands. *Oral Oncol*. 2018;82:29–33.
38. Ayre G, Hyrcza M, Wu J, et al. Secretory carcinoma of the major salivary gland: provincial population-based analysis of clinical behavior and outcomes. *Head Neck*. 2019;41:1227–1236.
39. Anderson JL, Haidar YM, Armstrong WB, et al. Analysis of clinical features of mammary analog secretory carcinoma using the Surveillance, Epidemiology, and End Results Database. *JAMA Otolaryngol Head Neck Surg*. 2019;145:91–93.
40. Alves LDB, de Melo AC, Farinha TA, et al. A systematic review of secretory carcinoma of the salivary gland: where are we? *Oral Surg Oral Med Oral Pathol Oral Radiol*. 2021;132:e143–e152.
41. Xu B, Viswanathan K, Umrau K, et al. Secretory carcinoma of the salivary gland: a multi-institutional clinicopathologic study of 90 cases with emphasis on grading and prognostic factors. *Histopathology*. 2022;81:670–679.
42. Sun J, Wang L, Tian Z, et al. Higher Ki67 index, nodal involvement, and invasive growth were high risk factors for worse prognosis in conventional mammary analogue secretory carcinoma. *J Oral Maxillofac Surg*. 2019;77:1187–1202.
43. Stanley RJ, Weiland LH, Olsen KD, et al. Dedifferentiated acinic cell (acinous) carcinoma of the parotid gland. *Otolaryngol Head Neck Surg*. 1988;98:155–161.
44. Skalova A, Leivo I, Hellquist H, et al. High-grade transformation/dedifferentiation in salivary gland carcinomas: occurrence across subtypes and clinical significance. *Adv Anat Pathol*. 2021;28:107–118.
45. Stevens TM, Kovalovsky AO, Velosa C, et al. Mammary analog secretory carcinoma, low-grade salivary duct carcinoma, and mimickers: a comparative study. *Mod Pathol*. 2015;28:1084–1100.
46. Majewska H, Skalova A, Stodulski D, et al. Mammary analogue secretory carcinoma of salivary glands: a new entity associated with ETV6 gene rearrangement. *Virchows Arch*. 2015;466:245–254.
47. Laco J, Svajdler M Jr, Andrejs J, et al. Mammary analog secretory carcinoma of salivary glands: a report of 2 cases with expression of basal/myoepithelial markers (calponin, CD10 and p63 protein). *Pathol Res Pract*. 2013;209:167–172.
48. Serrano-Arevalo ML, Mosqueda-Taylor A, Dominguez-Malagon H, et al. Mammary analogue secretory carcinoma (MASC) of salivary gland in four Mexican patients. *Med Oral Patol Oral Cir Bucal*. 2015;20:e23–e29.
49. Brandwein MS, Ivanov K, Wallace DI, et al. Mucoepidermoid carcinoma: a clinicopathologic study of 80 patients with special reference to histological grading. *Am J Surg Pathol*. 2001;25: 835–845.
50. Perzin KH, Gullane P, Clairmont AC. Adenoid cystic carcinomas arising in salivary glands: a correlation of histologic features and clinical course. *Cancer*. 1978;42:265–282.
51. Szanto PA, Luna MA, Tortoledo ME, et al. Histologic grading of adenoid cystic carcinoma of the salivary glands. *Cancer*. 1984;54: 1062–1069.
52. Spiro RH, Huvos AG, Strong EW. Adenoid cystic carcinoma of salivary origin. A clinicopathologic study of 242 cases. *Am J Surg*. 1974;128:512–520.
53. van Weert S, van der Waal I, Witte BI, et al. Histopathological grading of adenoid cystic carcinoma of the head and neck: analysis of currently used grading systems and proposal for a simplified grading scheme. *Oral Oncol*. 2015;51:71–76.
54. Skálová A, Bell D, Bishop JA, et al. Secretory carcinoma. In: El-Naggar A, Chan JKC, Grandis JR, Takata T, Slootweg PJ, eds. *World Health Organization (WHO) Classification of Head and Neck Tumours*, 4th ed. IARC Press ; 2017:177–178.
55. Vander Poorten V, Triantafyllou A, Thompson LD, et al. Salivary acinic cell carcinoma: reappraisal and update. *Eur Arch Otorhinolaryngol*. 2016;273:3511–3531.
56. Patel NR, Sanghvi S, Khan MN, et al. Demographic trends and disease-specific survival in salivary acinic cell carcinoma: an analysis of 1129 cases. *Laryngoscope*. 2014;124:172–178.
57. Boukheris H, Curtis RE, Land CE, et al. Incidence of carcinoma of the major salivary glands according to the WHO classification, 1992 to 2006: a population-based study in the United States. *Cancer Epidemiol Biomarkers Prev*. 2009;18:2899–2906.
58. Chiosea SI, Griffith C, Assaad A, et al. The profile of acinic cell carcinoma after recognition of mammary analog secretory carcinoma. *Am J Surg Pathol*. 2012;36:343–350.
59. Khalele BA. Systematic review of mammary analog secretory carcinoma of salivary glands at 7 years after description. *Head Neck*. 2017;39:1243–1248.